



# Developing surrogate indicators for predicting suppression of halophenols formation potential and abatement of estrogenic activity during ozonation of water and wastewater

Yu Huang<sup>a</sup>, Shi Cheng<sup>a</sup>, Ya-Ping Wu<sup>a</sup>, Ji Wu<sup>a</sup>, Yan Li<sup>a</sup>, Zong-Li Huo<sup>b</sup>, Ji-Chun Wu<sup>c</sup>, Xian-Chuan Xie<sup>a, \*\*</sup>, Gregory V. Korshin<sup>d</sup>, Ai-Min Li<sup>a</sup>, Wen-Tao Li<sup>a, c, \*</sup>

<sup>a</sup> State Key Laboratory of Pollution Control and Resources Reuse, School of the Environment, Nanjing University, Nanjing, 210023, China

<sup>b</sup> Jiangsu Provincial Center for Disease Control and Prevention, Nanjing, 210023, China

<sup>c</sup> Key Laboratory of Surficial Geochemistry Ministry of Education, School of Earth Sciences and Engineering, Hydrosiences Department, Nanjing University, Nanjing, 210023, China

<sup>d</sup> Department of Civil and Environmental Engineering, University of Washington, Seattle, WA, USA

## ARTICLE INFO

### Article history:

Received 7 March 2019

Received in revised form 18 May 2019

Accepted 26 May 2019

Available online xxx

### Keywords:

Ozonation

Dissolved organic matter

Halophenol

Endocrine disrupting chemical

Surrogate indicator

Haloacetic acids

## ABSTRACT

This study focused on developing surrogate indicators for predicting oxidation of phenolic groups in dissolved organic matter (DOM), suppression of halophenols' formation potential and abatement of estrogenic activity during ozonation of water and wastewater. The evolution of pH-dependent differential absorbance spectra suggests that O<sub>3</sub> preferentially reacts with the DOM phenolic moieties and less so with the aromatic carboxylic groups with increasing O<sub>3</sub>/DOC (dissolved organic carbon) ratios and changes of UV absorbance and fluorescence. When ozonation used as pretreatment, the formation of halophenols in subsequent chlorination decreased linearly with increasing O<sub>3</sub> doses or changes of UV absorbance until it reached 85% suppression of the halophenols' formation from unaltered DOM. The thresholds of decreases of UVA<sub>254</sub>, UVA<sub>280</sub> and humic-like fluorescence corresponding to 85% suppression of halophenols' formation were in the range of 25%–30%, 30%–35% and 30%–45%, respectively. Pre-ozonation also showed a moderate suppression of haloacetic acids (HAAs) formation potentials, ≤26.5% for reverse osmosis isolate of Suwannee River natural organic matter and ≤31.5% for Yangtze River at applied O<sub>3</sub> doses. Measurement of changes of estrogenic activity during ozonation of water and wastewater showed that to attain a >90% abatement of estrogenic activity, the corresponding thresholds of decreases of UVA<sub>254</sub>, UVA<sub>280</sub> and humic-like fluorescence were ~30%, ~40%, and ~70%, respectively. Bromate formation was also suppressed to below 10 μg/L before these thresholds. This study suggests that optimal ozonation conditions and a balance between control of disinfection byproducts (halophenols, HAAs and bromate) and elimination of estrogenic activity can be reached based on online data.

© 2019.

## 1. Introduction

Ozonation has been widely employed in many full-scale water and wastewater treatment plants due to its good performances in removal of odor, color and various organic micropollutants, its broadband action against many pathogens, and its maturity and relatively low energy demand (Gerrity and Snyder, 2011; von Gunten, 2003a; b, 2018). Meanwhile, chlorination is the most widely used disinfection process due to its inexpensive cost and ability of continuous disinfection.

However, the presence of dissolved organic matter (DOM) in water and wastewater is a significant sink for chemical oxidants and

tends to lower the efficiency of oxidation and disinfection (Aeschbacher et al., 2012; Chon et al., 2015; Wenk et al., 2013). Much of this is due to oxidation of phenolic moieties in DOM. Phenolic moieties including mono- and poly-hydroxylated benzene units with different substituents on the phenolic rings have been suggested to be the major components that define the antioxidant properties, UV absorbance and fluorescence spectra of DOM (Aeschbacher et al., 2012; Barsotti et al., 2016; Hernes et al., 2009; Korshin et al., 1997). Reactions between DOM-phenolic moieties and ozone can form a number of toxic organic byproducts (e.g., benzoquinones, hydroquinones, cyclic  $\alpha$ ,  $\beta$ -unsaturated ketones and substituted catechols) and assimilable organic carbon (Liu et al., 2015; Ramseier and von Gunten, 2009). DOM might react with chlorine or bromine species by oxidation or electrophilic aromatic substitution that results in the generation of trihalomethanes (THMs) and haloacetic acids (HAAs) (Criquet et al., 2015; Galapate et al., 2001; Oh et al., 2006). On the other hand, the electrophilic aromatic substitution reactions

\* Corresponding author. State Key Laboratory of Pollution Control and Resources Reuse, School of the Environment, Nanjing University, Nanjing, 210023, China.

\*\* Corresponding author.

Email addresses: [liwentao@nju.edu.cn](mailto:liwentao@nju.edu.cn) (X-C Xie); [xchxie@nju.edu.cn](mailto:xchxie@nju.edu.cn) (W-T Li)

between chlorine/bromine and DOM-phenolic moieties might also yield halophenols (Criquet et al., 2015). Although the concentrations of halophenols in drinking water have been found to be in ng/L level (Pan et al., 2017), these types of aromatic disinfection byproducts are more toxic than the regulated THMs and HAAs (Yang and Zhang, 2013). In addition, bromophenols have been shown to cause off-flavors in drinking water because their taste and odor thresholds are in the range of sub-ng/L to  $\mu\text{g/L}$  (Acero et al., 2005). Thus, oxidation of DOM-phenolic moieties might be a strategy for controlling DBPs formation potentials in subsequent chlorination, especially for those halophenols.

There are also increasing concerns related to the fate of endocrine disrupting chemicals (EDCs) because they have been shown to produce endocrine disruption in aquatic organisms at sub-ng/L trace level while most EDCs are not well removed by coagulation or biological treatment (Maniero et al., 2008; Westerhoff et al., 2005). Extensive studies in lab-, pilot- and full-scale conditions have shown that ozonation results in significant elimination of those phenolic-containing micropollutants including EDCs (Chon et al., 2015; Lee et al., 2013; Nakada et al., 2007). Some byproducts of EDCs degradation by ozonation might also be estrogenic, and their generation as well as the abatement of estrogenic activity has been relatively less studied. In addition, ozone has inherently high reactivity with most microorganisms (such as *E. coli*, *Bacillus subtilis* spores, and *Cryptosporidium parvum* oocysts) (Lee et al., 2016; von Gunten, 2003b). Whether the presence of bacteria in water and wastewater affects the oxidation of EDCs remains unclear and requires further investigation.

For suppression of halophenols formation and abatement of estrogenic activity, there is a trade-off between oxidation efficiency and energy consumption during ozonation of water and wastewater. A number of indicators deemed to be suitable for optimizing ozone doses have been proposed. These are based on  $\text{O}_3/\text{DOC}$  (dissolved organic carbon) mass ratio, differential UV absorbance (e.g.,  $\Delta\text{UVA}_{254}$  &  $\text{UVA}_{280}$ ), differential total/component fluorescence (e.g.,  $\Delta\text{TF}$ ) and electron donating capacity (Chon et al., 2015; Gerrity et al., 2012; Li et al. 2016, 2017; Wu et al., 2018). For online measurements, UV absorbance and fluorescence indices are most applicable, since miniaturized UV absorbance and fluorescence spectroscopy prototypes and deployment-ready devices that use UV light emitting diode have been developed (Li et al., 2016; Tedetti et al., 2013). In recent years, these spectroscopic indices have been studied as surrogate indicators for predicting the abatement of micropollutants, microbial inactivation, formation of bromate and assimilable organic carbon (Gerrity et al., 2012; Lee et al., 2016; Li et al. 2016, 2017; Nanaboina and Korshin, 2010; Wu et al., 2018). In this context, further research is needed to establish relationships between these and/or other spectroscopic indices indicative changes of the phenolic moieties in DOM caused by ozonation and, on the other hand, effects of ozonation on halophenols and other EDCs and their estrogenic activity.

The main objectives of this study were to apply relevant spectroscopic indicators to quantify three issues pertinent to the engagement of DOM phenolic moieties during ozonation: (i) changes of the phenolic moieties' abundance in DOM, (ii) suppression of halophenols' formation potential in post-chlorination of ozonated DOM, and (iii) abatement of EDCs and their estrogenic activity. This study suggests that optimal ozonation conditions and a balance between control of disinfection byproducts (halophenols, HAAs and bromate) and elimination of estrogenic activity can be reached based on online data.

## 2. Material and methods

### 2.1. Chemicals and reagents

For halophenols analysis, 2,4,6-trichlorophenol, 2,4,6-tribromophenol, 3,5-dichloro-4-hydroxybenzoic acid, 3,5-dichlorosalicylic acid, 3,5-dibromo-4-hydroxybenzoic acid, and 3,5-dibromosalicylic acid were purchased from Sigma-Aldrich. The EDCs standards, including estrone (E1, 99%), 17 $\beta$ -estradiol (E2, 97.0%), estriol (E3, 99.0%) and bisphenol A (BPA, 99.9%) were purchased from Tokyo Chemical Industry, and 17 $\alpha$ -ethinyl estradiol (EE2, 98%) purchased from Sigma-Aldrich. Isotopic labelled bisphenol A-d16 (BPA-d16, 98% from Sigma-Aldrich) was used as the internal standard for LC-MS/MS analyses of EDCs and halophenols.

The *E. coli* strain (ATCC 8099) was purchased and cultivated in the lab to prepare the *E. coli* suspension following the method described by Wu et al. (2018). Unless otherwise noted, other chemicals were used at least reagent grade purity, and all solutions were prepared in ultrapure water (18.2 M $\Omega$ /cm).

### 2.2. NOM isolates, water and wastewater samples

The reverse osmosis isolate of Suwannee River NOM (SR\_NOM, Catalog No. 2R101N, from International Humic Substances Society) was purchased for preparation of DOM solutions. Surface water sample (DOC 1.6–2.2 mg/L) was collected three times from the Yangtze River in Nanjing, and secondary wastewater effluent sample (DOC 3.0 mg/L) was collected from Nanjing Dachang wastewater treatment plant (WWTP-DC), which uses the conventional A<sup>2</sup>/O process. Another natural water sample was taken from Lake Pleasant (LP), Bothell, WA. LP water has a high DOC concentration ( $\sim 15$  mg/L) and UV<sub>254</sub> absorbance ( $\sim 0.73$  cm<sup>-1</sup>) (Li et al., 2017). These and other relevant water quality parameters are summarized in Table S1.

### 2.3. Batch ozonation and chlorination experiments

Ozone stock solution ( $\sim 60$  mg/L) was obtained by bubbling ice cooled ultrapure water with ozone gas, and spectrophotometrically standardized at  $\lambda = 258$  nm ( $\epsilon_{258\text{nm}, \text{O}_3} = 3000 \text{ M}^{-1} \text{ cm}^{-1}$ ) every time it was prepared. In ozonation batch experiments, requisite volume of the ozone stock solution was dosed into water samples to reach a desired value of specific  $\text{O}_3$  dose ( $\text{O}_3/\text{DOC}$  mass ratios were in the range of 0–1.7 mg/mg). Ozonation was carried out at room temperature, and samples were gently shaken in capped bottle until the residual ozone naturally decayed for 1 h. UV absorbance and fluorescence measurements were done for all samples, and the fluorescence excitation and emission matrixes are provided in Fig. S1. The conditions of all the batch ozonation and chlorination experiments were summarized in Table S2.

For studying changes of DOM-phenolic moieties, the working solutions of SR\_NOM with a 3.0 mg/L DOC concentration were prepared and transferred into 100 mL clean sterilized glass bottles. After ozonation, 50 mL of each sample was taken for pH-titration differential absorbance spectra (DAS) analysis. The pH-titration DAS analyses for Yangtze River and WWTP-DC failed due to formation of calcite or struvite-like turbidity at pH > 8.

For assessing effects of pre-ozonation on the formation of halophenols and HAAs during post-chlorination, the working solutions of SR\_NOM (3.0 mg/L as DOC) and Yangtze River were prepared by spiking 100  $\mu\text{g/L}$  Br<sup>-</sup> and 5 mM pH = 7 phosphate buffer. Each 400 mL of the working solutions was transferred into a 500 mL

clean glass bottle for pre-ozonation. After ozone naturally decayed, a 300 mL aliquot of the ozonated working solution was transferred into another clean glass bottle. To examine effects of post-chlorination, the ozonated SR\_NOM solution was spiked with 5 mg/L of free available chlorine (FAC). Chlorine was dosed using hypochlorite solution which was spectrophotometrically standardized at  $\lambda=292\text{ nm}$  ( $\epsilon_{292\text{ nm}}$ ,  $\epsilon_{\text{FAC}}=350\text{ M}^{-1}\text{ cm}^{-1}$ ) (Forsyth et al., 2013). The concentration of residual FAC was measured by DPD colorimetry ( $\lambda=515\text{ nm}$ ) immediately after taking 1 mL samples at specific contact times. After 24 h FAC exposure, the residual FAC was quenched with requisite amount of thio-sulfate. During the post-chlorination of ozonated WWTP-DC wastewater, significant formation of flocs was observed after FAC was dosed. Thus the effect of pre-ozonation on the formation of halophenols was not evaluated for WWTP-DC wastewater. After chlorination, 1 mL of each sample was taken for HAAs analysis and 250 mL of each sample was taken for solid phase extraction of halophenols.

To evaluate effects of ozone on the abatement of EDCs and their estrogenic activity, the working solution of SR\_NOM (2.5 mg/L as DOC) was spiked with 500 ng/L EDCs, 100  $\mu\text{g/L Br}^-$  and 5 mM pH=7 phosphate buffer. The working solution of Yangtze River and DC wastewater with or without *E.coli* ( $\sim 10^5\text{ cell/mL}$ ) was also spiked with 500 ng/L EDCs, 100  $\mu\text{g/L Br}^-$  and 5 mM pH=7 phosphate buffer. The spiked *E.coli* concentration was according to autochthonous bacteria concentration of unfiltered Yangtze River and WWTP-DC effluent measured by flow cytometer, which were in the range of  $10^5\sim 10^6\text{ cell/mL}$  (Wu et al., 2018). Each 300 mL aliquot of the working solutions was transferred into a 500 mL clean glass bottle for ozonation. After ozone naturally decayed, each 250 mL aliquot of the ozonated working solution was transferred into another clean bottle for solid phase extraction and EDCs analysis.

## 2.4. Analytical methods

### 2.4.1. The pH-titration DAS for quantitative analysis of phenolic groups in DOM

As the method described by Dryer et al. (2008) and Young et al. (2018), about 40 mL of raw or treated DOM solutions was acidified to pH  $\sim 3.0$  with 1 M  $\text{HClO}_4$ , and then gradually titrated adding requisite amounts of NaOH solutions (1 M, 2 M and 5 M) to increase a final ca. 10.2 pH value. The absorbance spectra were recorded upon stabilization of each pH, using a 5 cm quartz cell and a Shimadzu UV2700 spectrophotometer. DAS were calculated using the following equation:

$$\Delta A_{pH(\lambda)} = \frac{A_{pH(\lambda)} - A_{pH\_Ref(\lambda)}}{l_{cell} \times DOC}, L \cdot \text{mg}^{-1} \cdot \text{cm}^{-1}$$

In this equation, the cell length  $l_{cell}$  is 5 cm, and the DOC concentration is 3 mg/L for both SR\_NOM solution and diluted LP surface water;  $A_{pH(\lambda)}$  is the absorbance measured from 200 to 600 nm at varied pH; and  $A_{pH\_Ref(\lambda)}$  is the reference absorbance spectra acquired at pH  $\sim 3.0$ .

### 2.4.2. LC-MS/MS method for halophenols and EDCs

Halophenols and EDCs were concentrated by solid phase extraction using Oasis HLB cartridge, as described in the supporting information section, **Text S1**. The recovery rates for halophenols and EDCs are listed in Table S3.

LC-MS/MS analyses were carried out on an Agilent Infinity 1290 LC system coupled to ABSciex 5500 triple quadrupole mass spec-

trometer (ABSciex, MA, USA). Chromatographic separation was performed using Waters<sup>®</sup> BEH C18 reversed phase column ( $2.1 \times 100\text{ mm}$ ,  $1.7\text{ }\mu\text{m}$ ). Ultrapure water (Solvent A) and methanol (LC-MS grade) (Solvent B) were used as the mobile phase, as shown in Table S4 for halophenols and Table S5 for EDCs. The optimized MRM parameters for targeted halophenols and EDCs were summarized in Table S6 and Table S7, respectively. The injection volume was 10.0  $\mu\text{L}$  and the flow rate was 0.3 mL/min. For all targeted chemicals, the MS/MS detection was performed in the negative ion mode. All measurements were taken in duplicate, and the results were presented as mean values  $\pm$  STD.

### 2.4.3. LC-MS/MS method for bromate and HAAs

Haloacetic acids and bromate were determined simultaneously using a non-suppressed ion chromatography with electrospray ionization-tandem mass spectrometry (Wu et al., 2018). The IC-ESI-MS/MS method also works on the Agilent 1290 series HPLC system coupled with an QTRAP<sup>®</sup> 5500 LC-MS/MS operating with negative mode electrospray ionization. Separation was performed using an ion exchange column Dionex IonPac AS-16 under isocratic conditions with a mobile phase comprising 30% of a 1 M aqueous methylamine solution (Solvent A) and 70% of acetonitrile (Solvent B) at a flow rate of 0.30 mL/min for separation. This method utilizes the direct injection of 10  $\mu\text{L}$  volumes of 0.22  $\mu\text{m}$  membrane-filtered aqueous samples without the need for pre-extraction, derivatization or concentration procedures.

### 2.4.4. Estrogenic activity analysis

Estrogenic activity was evaluated using the yeast two-hybrid (YES) assay of CASA-Estrogen (Aquality Technology, Wuxi, China). In this assay, yeast was transcribed with human estrogen receptor- $\alpha$  (hER $\alpha$ ) and  $\beta$ -galactosidase was induced by estrogenic chemicals in water samples (Routledge and Sumpter, 1996). E2 was used as a positive control, and pure water was used as a negative control. The estrogenic activities of water samples determined by the YES assay were represented as E2 equivalent values (EEQ). Although the YES is reported less sensitive than the available reporter gene assays based on mammalian cells, it is applicable to the working solutions spiked with EDCs in this study (Leusch et al. 2010, 2017).

## 3. Results and discussion

### 3.1. Changes of DOM-phenolic moieties

The pH titrations of SR\_NOM solution showed that for the wavelength range of 240–450 nm, consistent and monotonic increases of the absorbance spectra were observed for increasing pHs (Fig. S2). This is primarily associated with changes of the electron-transfer (ET) transitions in a variety of aromatic chromophores characteristic for DOM (Korshin et al., 1997). The deprotonation at increasing pHs of the phenolic and aromatic carboxylic functional groups in DOM changes their electronic properties and, as a result electronic transitions in DOM molecules. These changes can be quantified via pH-differential absorbance spectra (Dryer et al., 2008). Consistent with recent literature (Young et al., 2018), the pH differential spectra of SR\_NOM and LP\_NOM (Fig. S3a and Fig. S4, respectively) exhibit two features: a narrow band centered at  $\sim 280\text{ nm}$  (DA280) associated with aromatic carboxylic acid groups, and a broad band centered at  $\sim 340\text{ nm}$  (DA340) that is primarily associated with phenolic moieties. The DA340/DA280 ratio, which was determined when pH was changed from pH $\sim 3.0$  to pH $\sim 10.2$ , was proposed as an indicator

reflecting the relative abundance of phenolic moieties over the aromatic carboxylic functional groups.

Fig. 1 depicts changes of the DA340/DA280 ratio normalized by the data of non-treated SR\_NOM as a function of  $O_3$ /DOC ratio, decrease of UV absorbance, decrease of humic-like fluorescence in three batches of SR\_NOM ozonation experiments. At low  $O_3$  doses ( $O_3$ /DOC < 0.2), the absolute intensity of UVA254, UVA280, and humic-like fluorescence slightly decreased with an extent of 10%~20% inferred from the X-axis value of the related points in Fig. 1b–d, and apparently the destruction of aromatic moieties resulted in decreases of UV absorbance and fluorescence. However, the DA340/DA280 ratios slightly increased in these conditions, suggesting that the relative abundance of the protonation-active phenolic moieties vs aromatic carboxylic functional groups increased. Tentscher et al. (2018) recently reported that ozonation of para-substituted phenolic compounds yields *p*-benzoquinones, cyclic  $\alpha,\beta$ -unsaturated ketones, and substituted catechols. For most model phenolic compounds, catechol yields were relatively high at low ozone doses ( $[O_3]/[phenol] < 0.3$ ) and decreased with increasing ozone doses (Tentscher et al., 2018). Thus, the increases of the relative abundance of phenolic moieties versus aromatic carboxylic groups as indicated by the corresponding DA340/DA280 values decreased prominently from >1.0 to the range of 0.6–0.8. The corresponding decreases of UVA254, UVA280 and humic-like fluorescence were less than 25%, 35%, and 45%, respectively. At higher  $O_3$  doses, although the UV absorbance and humic-like fluorescence further decreased, the normalized DA340/DA280 ratios generally remained in the range of 0.6–0.8. Consistently, with  $O_3$ /DOC > 0.5, the DAS of SR\_NOM solutions exhibited similar contour profiles (Fig. S3).

Examination of the DAS data for LP surface water further confirmed that ozonation treatment resulted in consistent decreases of the relative abundance of the phenolic versus carboxylic moieties in DOM (Fig. S4).

### 3.2. Effect of pre-ozone on suppression of DBPs formation potential during chlorination

#### 3.2.1. Suppression of halophenolic DBPs formation

Phenolic moieties in NOM react with chlorine or bromine species either by electron transfer or by electrophilic aromatic substitution process, leading to the formation of aromatic or aliphatic DBPs.

Fig. 2 shows the formation potentials of halophenolic DBPs generated during chlorination of the pre-ozonated SR\_NOM and Yangtze River samples. In the case of chlorination of SR\_NOM (DOC ~3.0 mg/L &  $[Br^-] \sim 100 \mu\text{g/L}$ ) buffered at pH=7, 3,5-dibromosalicylate acid was the predominant species of the target halophenols (~73 ng/L), followed by 3,5-dichlorosalicylate acid (~34 ng/L). Results for the chlorination of Yangtze River sample (DOC ~2.2 mg/L &  $[Br^-] > 100 \mu\text{g/L}$ ) buffered at pH=7 showed that 3,5-dibromosalicylate acid was still the predominant species (~52 ng/L) but much less of 3,5-dichlorosalicylate acid (~4 ng/L) was formed compared with the data for SR\_NOM. The differences in the abundance of halophenol species between SR\_NOM and Yangtze River should be attributed to their differences in  $[Br^-]/[\text{reactive DOC}]$ . With increasing initial  $[Br^-]/[\text{reactive DOC}]$ , the proportions of the chlorophenols should be decreased, because bromine is more reactive with phenolic compounds than chlorine ( $k_{HOBr}/k_{HOCl} \approx 3000$ ) (Criquet et al., 2015). In addition to humic substances that dominate SR\_NOM, Yangtze River DOM is likely to contain higher contributions of relatively less reactive components operationally referred to as proteinaceous biopolymers, building blocks and small aliphatic

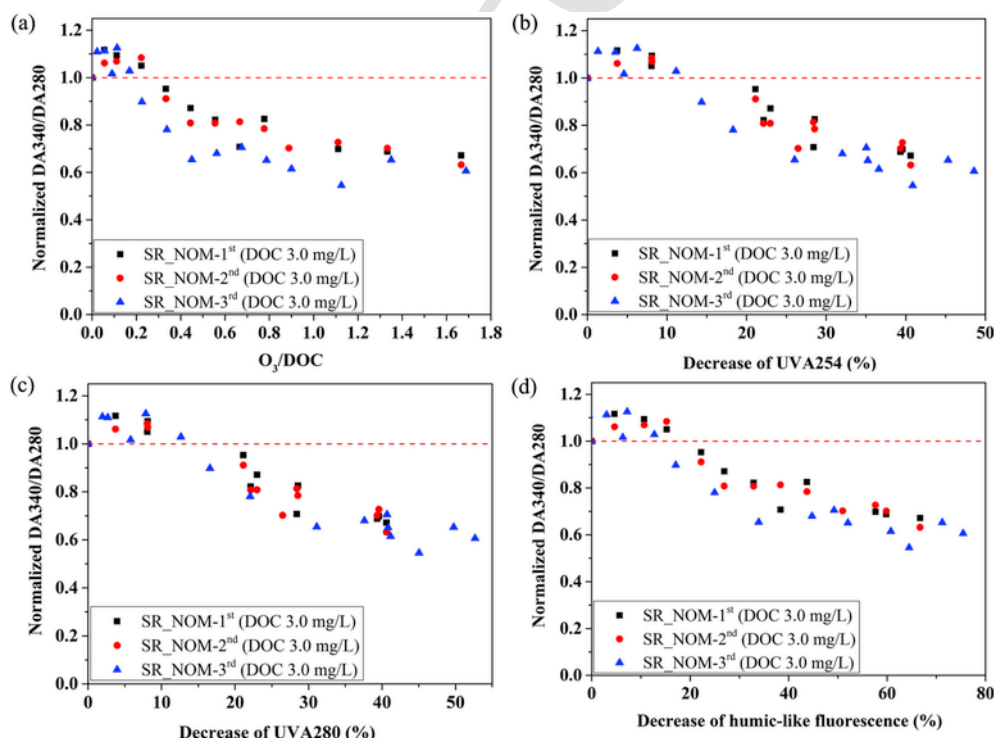


Fig. 1. Changes of the normalized DA340/DA280 ratios of SR\_NOM at pH~10.2 as a function of (a)  $O_3$ /DOC mass ratio, (b) decrease of UVA254, (c) decrease of UVA280 and (d) decrease of humic-like fluorescence in three batches of ozonation experiments.

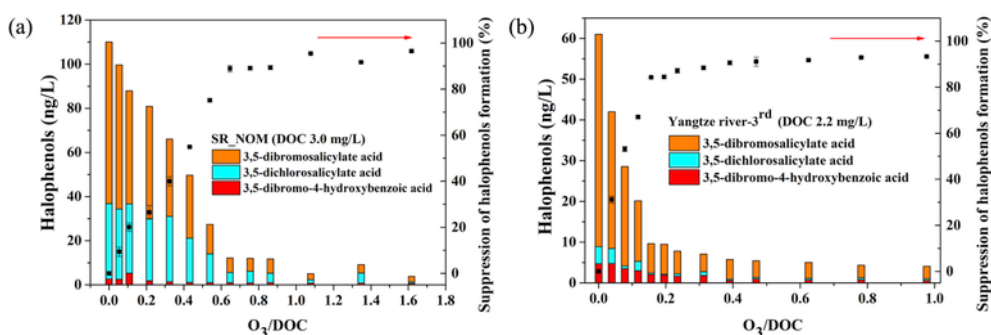


Fig. 2. Formation potentials (left axis) and relative suppression (right axis) of halophenolic DBPs during post-chlorination of (a) SR\_NOM and (b) Yangtze River samples versus specific  $O_3$  doses.

molecules (Huber et al., 2011). The formation potentials of 3,5-dibromo-4-hydroxybenzoic acid was also relatively low. A plausible explanation might be that natural DOM contains more salicylic moieties than 4-hydroxybenzoic moieties.

The other targeted halophenols including 2,4,6-trichlorophenol, 2,4,6-tribromophenol and 3,5-dichloro-4-hydroxybenzoic acid showed low recovery rates during solid phase extraction (Table S3), and thus their formation potentials are not presented in Fig. 2. Prior studies that examined the chlorination of seawater spiked with 0.25, 0.5, and 1 mg/L phenol found that 2,4,6-tribromophenol was the predominant species in such conditions (25.8, 172.4, and 687.4  $\mu\text{g/L}$ , respectively) (Ding et al., 2018). However, in this study, the concentration of 2,4,6-tribromophenol was much less, i.e.,  $\sim 17$  ng/L for SR\_NOM and  $\sim 8$  ng/L for Yangtze River.

The total formation potential of halophenols in Fig. 2 gradually decreased nearly linearly as a function of specific  $O_3$  doses, until 85% of formation potential was suppressed (SR\_NOM,  $R^2=0.984$ ; Yangtze River,  $R^2=0.971$ , Table S8). The specific  $O_3$  doses corresponding to 85% suppression of halophenol formation for SR\_NOM and Yangtze River were at  $O_3/\text{DOC}\sim 0.6$  or  $O_3/\text{DOC}\sim 0.2$ , respectively. Over the threshold of 85% suppression, increasing  $O_3$  doses contributed less than 10% suppression of halophenols' formation.

Fig. 3 further demonstrates the suppression of formation potentials of individual and total halophenols versus the decreases of UVA254, UVA280 and humic-like fluorescence. These plots also exhibited two stages with different slopes. Before 85% suppression of halophenols' formation, there were also good linear correlations between suppression of halophenols' total formation potential and decreases of UVA254 or UVA280 ( $R^2>0.95$ ), as listed in Table S8. The thresholds of decreases of UVA254, UVA280 and humic-like fluorescence corresponding to 85% suppression of halophenols' formation were in the range of 25%–30%, 30%–35% and 30%–45%, respectively. It suggests that measurements of the decrease of UV absorbance is advantageous compared with the measurements of the decrease of fluorescence for indicating the suppression of halophenols' formation by pre-ozonation.

### 3.2.2. Suppression of HAAs

Fig. 4 shows the behavior of the formation potentials of HAAs formed in the case of chlorination of the pre-ozonated SR\_NOM and Yangtze River samples. The data demonstrate that the main HAA species were TCAA, BDCAA and BCAA during chlorination of both SR\_NOM and Yangtze River samples. For low ozone doses applied to both SR\_NOM ( $O_3/\text{DOC}<0.4$ ) and Yangtze River ( $O_3/\text{DOC}<0.1$ ), the HAAs formation potentials slightly increased (SR\_NOM) or minimally decreased (Yangtze River), while over 50% halophenols' formation potential could be suppressed at such  $O_3$  doses. As shown in

Fig. 1, low  $O_3$  doses slightly decreased the aromatic chromophores and/or fluorophores, while on the other hand this may result in the formation of some by-products (e.g., hydroquinone, catechol moieties) that are also important precursors of HAAs (Oh et al., 2006). With further increases of  $O_3$  doses, the HAAs formation potentials gradually decreased, especially those of TCAA and BDCAA. For the applied  $O_3$  doses, pre-ozonation resulted in a moderate suppression of HAAs formation potentials,  $\leq 26.5\%$  for SR\_NOM and  $\leq 31.5\%$  for Yangtze River.

### 3.3. Abatement of EDCs and their estrogenic activity

#### 3.3.1. Removal of EDCs

Fig. 5 shows the removal of the total concentrations of the selected EDCs (E1, E2, E3, EE2 and BPA) as a function of  $O_3/\text{DOC}$  ratio, decreases of UVA254, UVA280 and humic-like fluorescence. The results obtained for each individual EDC in batch ozonation experiments with and without the presence of *E.coli* spiked in the solution are provided in Figs. S5–9. The data show that the removal of E1, E2, E3, EE2 and BPA showed similar trends and all these species can be efficiently removed at low  $O_3$  doses ( $O_3/\text{DOC}<0.2$ ) across the different DOM matrixes used in this study. This is in agreement with the results of prior research which has shown that phenolic micropollutants could be efficiently removed at low  $O_3$  doses (Gerrity et al., 2012; Lee et al., 2013). Chon et al. (2015) reported that  $>90\%$  removal of EE2 can be reached with  $O_3/\text{DOC}<0.2$  during the ozonation of wastewater effluents. This is related to the fact that the electron-donating capacities of phenolic-moieties in the examined phenolic micropollutants lead to their high reactivity with  $O_3$ , i.e., the reaction rates of phenolic micropollutants with  $O_3$  at  $\text{pH}=7$  are generally  $>10^5 \text{ M}^{-1}\text{s}^{-1}$  (Lee and von Gunten, 2012). Bacterial membranes have also been shown to have high reactivity with  $O_3$  in comparison with DOM (Wu et al., 2018). However, no significant differences were observed for the data of the batch ozonation experiments with and without the presence of  $\sim 10^5$  cell/mL *E.coli* bacteria. This further confirms that ozonation is very effective for the removal of EDCs in a wide range of water and wastewater matrixes.

The decreases of UVA254 and UVA280 corresponding to  $\sim 90\%$  removal of EDCs were  $\sim 15\%$  and  $\sim 20\%$ , respectively; while the decreases of humic-like fluorescence related to these inflection points were  $\sim 20\%$  for SR\_NOM and Yangtze River water matrixes and  $\sim 50\%$  for DC wastewater effluents. In accord with the results reported by Chon et al. (2015) and Gerrity et al. (2012),  $\sim 20\%$  elimination of UVA254, 50%–60% elimination of total fluorescence or  $\sim 50\%$  decreases in electron-donating capacity during ozonation of wastewater effluents was associated with  $>90\%$  elimination of EE2, BPA and other phenolic micropollutants.



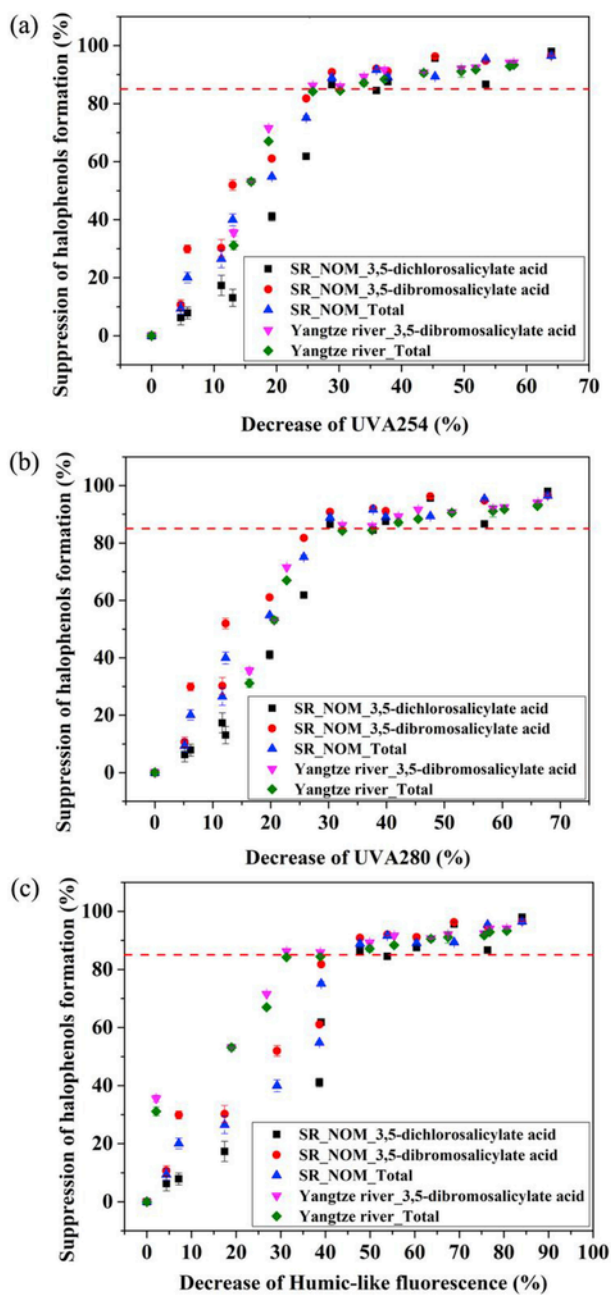


Fig. 3. Suppression of the formation potentials of individual halophenol species and total halophenols versus the decreases of (a) UVA254, (b) UVA280 and (c) humic-like fluorescence.

### 3.3.2. Abatement of estrogenic activity

In addition to the removal of the individual EDC species, changes of the estrogenic activity need to be quantified to make sure that it is also removed. Fig. 6a demonstrates the abatement of estrogenic activity measured by YES assay as a function of  $O_3/DOC$  ratios in different DOM matrixes. With low  $O_3$  doses ( $O_3/DOC < 0.20$ ), where the EDCs could be sufficiently removed, significant levels of residual estrogenic activity were still observed. At a 0.20 specific dose of  $O_3/DOC$ , the removal efficiencies of EEQ measured by YES assay were less than 80% for SR\_NOM and Yangtze River samples and were less than 60% for WWTP-DC samples. With increasing

$O_3/DOC$  ratios to  $\sim 0.35$  for SR\_NOM and Yangtze River and to  $\sim 0.50$  for WWTP-DC wastewater, over 90% of estrogenic activity were eliminated.

Fig. 7 compares the removal of the EEQ values measured by YES assay versus the calculated removal of EEQ across different matrixes. The EEQ calculation were carried out using Eq. (1) and the detected EDC concentrations. Contributions of the individual EDC species in the overall EEQ were estimated using the factors of the selected individual EDC reported in prior literature (Furuichi et al., 2004). The decrease of the calculated EEQ showed similar trends with each individual EDC (Fig. S10 vs Figs. S5–9). For the plots of the decrease of the measured EEQ values versus the decrease of the calculated EEQ, most dots were under the diagonal line, suggesting the abatement of estrogenic activity significantly lagged behind the oxidation of the parent EDCs and estrogenic intermediates may be formed at low  $O_3$  doses during ozonation. It might also arise from some unknown compounds in the environmental samples, either acting as estrogens and not being degraded by low-dose ozone, or compounds being transformed by ozone into more estrogenic compounds.

$$\text{Calculated EEQ} = 0.3 \times [E1] + 1 \times [E2] + 5.9 \times 10^{-3} \times [E3] + 2.2 \times [EE2] +$$

$$1.1 \times 10^{-4} \times [BPA] \quad (1)$$

Prior studies suggest that the presence of a phenolic ring contributes to the perfect bind of EDCs with estrogen receptor (Maniero et al., 2008). Among the selected EDCs, EE2, E2 and E1 mainly contribute to the estrogenic activity, as shown in Eq. (1). The oxidation of EE2, E2 and E1 occurs primarily at two reaction sites: a highly ozone reactive phenolic moiety ( $k \sim 3 \times 10^6 \text{ M}^{-1} \text{ s}^{-1}$  at pH=7) and a significantly less reactive ethynyl group of EE2,  $k \sim 200 \text{ M}^{-1} \text{ s}^{-1}$ , alcohol group of E2 or a keto group of E1 (Huber et al., 2004). This also suggests that at low  $O_3$  exposures, the phenolic moiety in the EDC will be mainly transformed. In this study, the phenolic ring of EDCs might still remain intact at low  $O_3$  doses ( $O_3/DOC < 0.2$ ); however, it might exist in the form of catechols, inferred from the results of model *para*-substituted phenols (Tentscher et al., 2018) and changes of the DA340/DA280 ratios of SR\_NOM (Fig. 1). Prior studies have also proposed or identified the catechol-like byproducts during oxidation of EE2, E2 and 5,6,7,8-tetrahydro-2-naphthol (Bila et al., 2007; Huber et al., 2004; Maniero et al., 2008; Ohko et al., 2002). According to Bila et al. (2007), 2-hydroxyestradiol and testosterone were identified as the oxidation byproducts of E2. Further verified by YES assay tests, 2-hydroxyestradiol showed estrogenic activity with an  $EC_{50}$  of  $2.10 \mu\text{g/L}$  whereas testosterone didn't (Bila et al., 2007). Additionally, Maniero et al. (2008) further proposed *estra-1,3,5(10)-trien-17-one,2,3-bis[(trimethyl)oxy]* and *estra-1,3,5(10)-trien-17-one,3,4-bis[(trimethyl)oxy]* as the oxidation byproducts of EE2, which might also exhibit estrogenic activity.

Results shown in Fig. 6 b-d demonstrate that, to assure a  $>90\%$  abatement of estrogenic activity, the corresponding decreases of UVA254, UVA280 and humic-like fluorescence should exceed the thresholds of  $\sim 30\%$ ,  $\sim 40\%$ , and  $70\%$ , respectively. At these thresholds, the formation bromate was still  $< 10 \mu\text{g/L}$  for both water and wastewater matrixes (Fig. S11). These and other results of this study demonstrates that it is possible to reach a compromise or balance between control of DBPs formation (halophenols, HAAs, and bromate) and elimination of estrogenic activity based on the application of

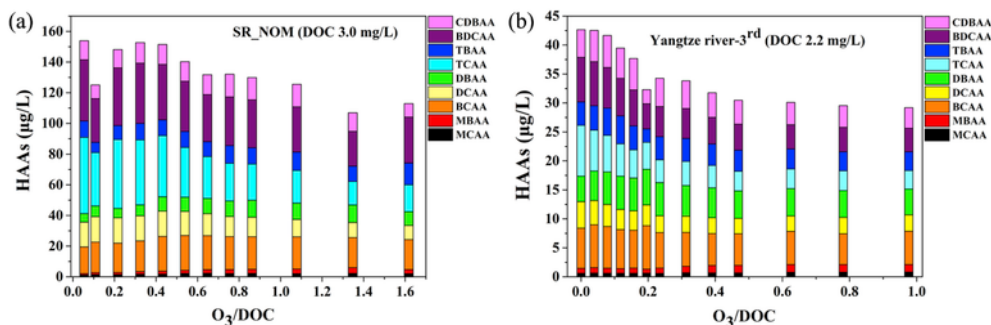


Fig. 4. Formation potentials of HAAs generated in post-chlorination of (a) SR\_NOM and (b) Yangtze River samples at varying  $O_3/DOC$  ratios.

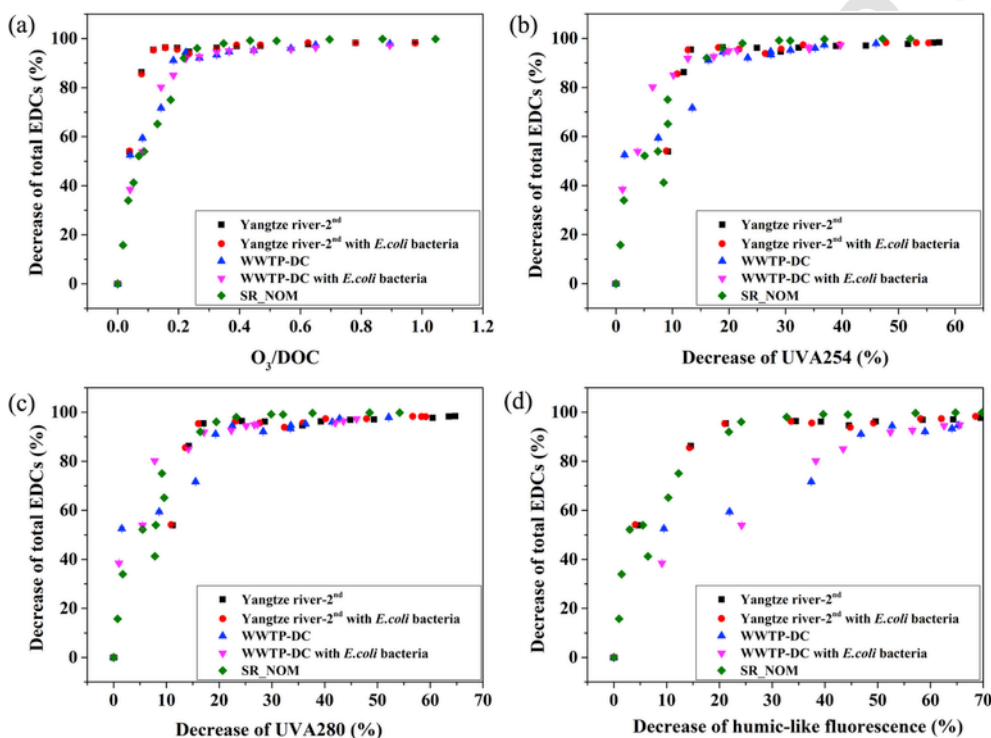


Fig. 5. Removal of the total concentrations of the selected EDCs as a function of (a)  $O_3/DOC$  ratio, (b) decreases of UVA254, (c) decreases of UVA280 and (d) humic-like fluorescence.

spectroscopic indicators that predicting the performance of oxidation and disinfection in ozonation.

#### 4. Conclusions

- The DA340/DA280 ratios determined via differential absorbance spectroscopic measurements in pH-titration analyses, can be used to quantify the evolution of the relative abundance of phenolic groups versus aromatic carboxylic groups during ozonation. These data show that while  $O_3$  preferentially reacts with DOM-phenolic moieties, applications of low  $O_3$  doses ( $O_3/DOC < 0.2$ ) cause the DA340/DA280 ratios to slightly increase; this effect may be related to the formation of catechol-like moieties.
- When ozonation used as pretreatment, the formation of halophenols in subsequent chlorination decreased linearly with  $O_3$  dose until it reached 85% level of suppression. The thresholds of decreases of UVA254, UVA280 and humic-like fluorescence corresponding to an 85% suppression of halophenols' formation were in

the range of 25%–30%, 30%–35%, and 30%–45%, respectively. Ozonation pretreatment caused the formation potentials of HAAs to increase slightly at low  $O_3$  doses, and high  $O_3$  doses were observed to result in mild decreases of the HAAs formation potentials,  $\leq 26.5\%$  for SR\_NOM and  $\leq 31.5\%$  for Yangtze River at applied  $O_3$  doses.

- During ozonation of water and wastewater, the abatement of estrogenic activity significantly lagged behind the elimination of EDCs. To assure a  $>90\%$  abatement of estrogenic activity, the corresponding decreases of UVA254, UVA280 and humic-like fluorescence had to be  $> \sim 30\%$ ,  $\sim 40\%$ , and  $\sim 70\%$ , respectively. At these thresholds, the formation bromate was still  $< 10 \mu\text{g/L}$  for both water and wastewater matrixes
- The use of  $O_3/DOC$  ratios or spectroscopic indicators allows reaching a compromise or balance between optimal controls of DBPs formation (halophenols, HAAs, and bromate) and the elimination of estrogenic activity of ozonated surface water and wastewater.

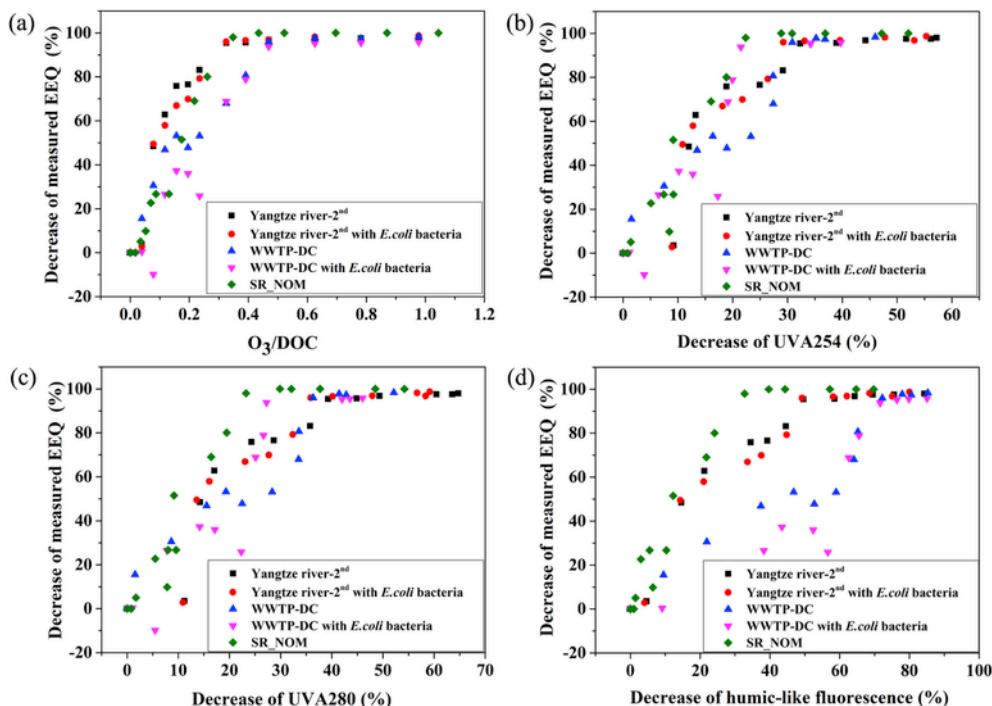


Fig. 6. Removal of the estrogenic activity measured by YES assay as a function of (a)  $O_3/DOC$  mass ratio, (b) decreases of UVA254, (c) UVA280 and (d) humic-like fluorescence.

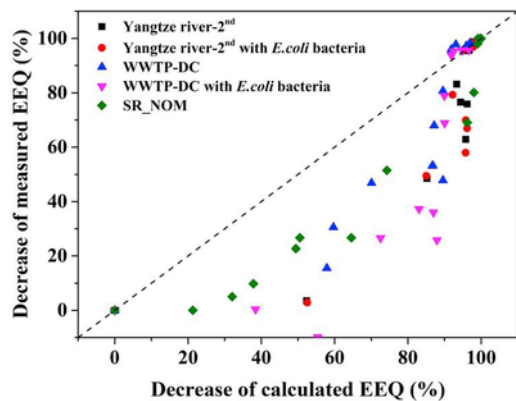


Fig. 7. Comparison of the removal of the YES assay measured EEQ values versus the calculated EEQ removal levels determined for different matrixes.

## Acknowledgement

This study was financially supported by National Natural Science Foundation of China (51708279&51438008), Basic Research Program of Jiangsu Province (BK20170642), and National Key R&D Program of China (2016YFE0112300) as well as its counterpart MADFORWATER Project (No. 688320) in the framework of European Horizon2020 Program. Dr. X.C. Xie also thanks the Major Science and Technology Program for Water Pollution Control and Treatment of China (2017ZX07602). The authors would like to thank staff in Jiangsu Provincial Center for Disease Control and Prevention and Jiangyin Environmental Protection Bureau for their help in EDCs, halophenols, HAAs and bromate analyses.

## Appendix A. Supplementary data

Supplementary data to this article can be found online at <https://doi.org/10.1016/j.watres.2019.05.092>.

## References

- Acero, J.L., Piriou, P., von Gunten, U., 2005. Kinetics and mechanisms of formation of bromophenols during drinking water chlorination: assessment of taste and odor development. *Water Res.* 39 (13), 2979–2993.
- Aeschbacher, M., Graf, C., Schwarzenbach, R.P., Sander, M., 2012. Antioxidant properties of humic substances. *Environ. Sci. Technol.* 46 (9), 4916–4925.
- Barsotti, F., Ghigo, G., Vione, D., 2016. Computational assessment of the fluorescence emission of phenol oligomers: a possible insight into the fluorescence properties of humic-like substances (HULIS). *J. Photochem. Photobiol. A Chem.* 315, 87–93.
- Bila, D., Montalvão, A.F., Azevedo, D.d.A., Dezotti, M., 2007. Estrogenic activity removal of 17 $\beta$ -estradiol by ozonation and identification of by-products. *Chemosphere* 69 (5), 736–746.
- Chon, K., Salhi, E., von Gunten, U., 2015. Combination of UV absorbance and electron donating capacity to assess degradation of micropollutants and formation of bromate during ozonation of wastewater effluents. *Water Res.* 81, 388–397.
- Criquet, J., Rodriguez, E.M., Allard, S., Wellauer, S., Salhi, E., Joll, C.A., von Gunten, U., 2015. Reaction of bromine and chlorine with phenolic compounds and natural organic matter extracts - electrophilic aromatic substitution and oxidation. *Water Res.* 85, 476–486.
- Ding, N., Sun, Y., Ye, T., Yang, Z., Qi, F., 2018. Control of halophenol formation in seawater during chlorination using pre-ozonation treatment. *Environ. Sci. Pollut. Res.* 25 (28), 28050–28060.
- Dryer, D.J., Korshin, G.V., Fabricino, M., 2008. In situ examination of the protonation behavior of fulvic acids using differential absorbance spectroscopy. *Environ. Sci. Technol.* 42 (17), 6644–6649.
- Forsyth, J.E., Zhou, P., Mao, Q., Asato, S.S., Meschke, J.S., Dodd, M.C., 2013. Enhanced inactivation of *Bacillus subtilis* spores during solar photolysis of free available chlorine. *Environ. Sci. Technol.* 47 (22), 12976–12984.
- Furuichi, T., Kannan, K., Giesy, J.P., Masunaga, S., 2004. Contribution of known endocrine disrupting substances to the estrogenic activity in Tama River water samples from Japan using instrumental analysis and in vitro reporter gene assay. *Water Res.* 38 (20), 4491–4501.



- Galapate, R.P., Baes, A.U., Okada, M., 2001. Transformation of dissolved organic matter during ozonation: effects on trihalomethane formation potential. *Water Res.* 35 (9), 2201–2206.
- Gerrity, D., Gamage, S., Jones, D., Korshin, G.V., Lee, Y., Pisarenko, A., Trenholm, R.A., von Gunten, U., Wert, E.C., Snyder, S.A., 2012. Development of surrogate correlation models to predict trace organic contaminant oxidation and microbial inactivation during ozonation. *Water Res.* 46 (19), 6257–6272.
- Gerrity, D., Snyder, S., 2011. Review of ozone for water reuse applications: toxicity, regulations, and trace organic contaminant oxidation. *Ozone Sci. Eng.* 33 (4), 253–266.
- Hernes, P.J., Bergamaschi, B.A., Eckard, R.S., Spencer, R.G.M., 2009. Fluorescence-based proxies for lignin in freshwater dissolved organic matter. *J. Geophys. Res.-Biogeo.* 114 (G4).
- Huber, M.M., Terres, T.A., von Gunten, U., 2004. Removal of estrogenic activity and formation of oxidation products during ozonation of 17 $\alpha$ -ethinylestradiol. *Environ. Sci. Technol.* 38 (19), 5177–5186.
- Huber, S.A., Balz, A., Abert, M., Pronk, W., 2011. Characterisation of aquatic humic and non-humic matter with size-exclusion chromatography - organic carbon detection - organic nitrogen detection (LC-OCD-OND). *Water Res.* 45 (2), 879–885.
- Korshin, G.V., Li, C.-W., Benjamin, M.M., 1997. Monitoring the properties of natural organic matter through UV spectroscopy: a consistent theory. *Water Res.* 31 (7), 1787–1795.
- Lee, Y., Gerrity, D., Lee, M., Bogeat, A.E., Salhi, E., Gamage, S., Trenholm, R.A., Wert, E.C., Snyder, S.A., von Gunten, U., 2013. Prediction of micropollutant elimination during ozonation of municipal wastewater effluents: use of kinetic and water specific information. *Environ. Sci. Technol.* 47 (11), 5872–5881.
- Lee, Y., Imminger, S., Czekalski, N., von Gunten, U., Hammes, F., 2016. Inactivation efficiency of *Escherichia coli* and autochthonous bacteria during ozonation of municipal wastewater effluents quantified with flow cytometry and adenosine tri-phosphate analyses. *Water Res.* 101, 617–627.
- Lee, Y., von Gunten, U., 2012. Quantitative structure–activity relationships (QSARs) for the transformation of organic micropollutants during oxidative water treatment. *Water Res.* 46 (19), 6177–6195.
- Leusch, F.D.L., de Jager, C., Levi, Y., Lim, R., Puijker, L., Sacher, F., Tremblay, L.A., Wilson, V.S., Chapman, H.F., 2010. Comparison of five in vitro bioassays to measure estrogenic activity in environmental waters. *Environ. Sci. Technol.* 44 (10), 3853–3860.
- Leusch, F.D.L., Neale, P.A., Hebert, A., Scheurer, M., Schriks, M.C.M., 2017. Analysis of the sensitivity of in vitro bioassays for androgenic, progestagenic, glucocorticoid, thyroid and estrogenic activity: suitability for drinking and environmental waters. *Environ. Int.* 99, 120–130.
- Li, W.-T., Cao, M.-J., Young, T., Ruffino, B., Dodd, M., Li, A.-M., Korshin, G., 2017. Application of UV absorbance and fluorescence indicators to assess the formation of biodegradable dissolved organic carbon and bromate during ozonation. *Water Res.* 111, 154–162.
- Li, W.-T., Majewsky, M., Abbt-Braun, G., Horn, H., Jin, J., Li, Q., Zhou, Q., Li, A.-M., 2016. Application of portable online LED UV fluorescence sensor to predict the degradation of dissolved organic matter and trace organic contaminants during ozonation. *Water Res.* 101, 262–271.
- Liu, C., Tang, X., Kim, J., Korshin, G.V., 2015. Formation of aldehydes and carboxylic acids in ozonated surface water and wastewater: a clear relationship with fluorescence changes. *Chemosphere* 125, 182–190.
- Maniero, M.G., Bila, D.M., Dezotti, M., 2008. Degradation and estrogenic activity removal of 17 beta-estradiol and 17 alpha-ethinylestradiol by ozonation and O(3)/H(2)O(2). *Sci. Total Environ.* 407 (1), 105–115.
- Nakada, N., Shinohara, H., Murata, A., Kiri, K., Managaki, S., Sato, N., Takada, H., 2007. Removal of selected pharmaceuticals and personal care products (PPCPs) and endocrine-disrupting chemicals (EDCs) during sand filtration and ozonation at a municipal sewage treatment plant. *Water Res.* 41 (19), 4373–4382.
- Nanaboina, V., Korshin, G.V., 2010. Evolution of absorbance spectra of ozonated wastewater and its relationship with the degradation of trace-level organic species. *Environ. Sci. Technol.* 44 (16), 6130–6137.
- Oh, B.S., Kim, K.S., Kang, J.W., 2006. Ozonation of haloacetic acid precursor using phenol as a model compound: effect of ozonation by-products. *Water Sci. Technol. Water Supply* 6 (2), 215–222.
- Ohko, Y., Iuchi, K.-i., Niwa, C., Tatsuma, T., Nakashima, T., Iguchi, T., Kubota, Y., Fujishima, A., 2002. 17 $\beta$ -Estradiol degradation by TiO<sub>2</sub> photocatalysis as a means of reducing estrogenic activity. *Environ. Sci. Technol.* 36 (19), 4175–4181.
- Pan, Y., Wang, Y., Li, A., Xu, B., Xian, Q., Shuang, C., Shi, P., Zhou, Q., 2017. Detection, formation and occurrence of 13 new polar phenolic chlorinated and brominated disinfection byproducts in drinking water. *Water Res.* 112, 129–136.
- Ramseier, M.K., von Gunten, U., 2009. Mechanisms of phenol ozonation-kinetics of formation of primary and secondary reaction products. *Ozone Sci. Eng.* 31 (3), 201–215.
- Routledge, E.J., Sumpter, J.P., 1996. Estrogenic activity of surfactants and some of their degradation products assessed using a recombinant yeast screen. *Environ. Toxicol. Chem.* 15 (3), 241–248.
- Tedetti, M., Joffr e, P., Goutx, M., 2013. Development of a field-portable fluorometer based on deep ultraviolet LEDs for the detection of phenanthrene- and tryptophan-like compounds in natural waters. *Sensor. Actuator. B Chem.* 182, 416–423.
- Tentscher, P.R., Bourgin, M., von Gunten, U., 2018. Ozonation of para-substituted phenolic compounds yields p-benzoquinones, other cyclic  $\alpha,\beta$ -unsaturated ketones, and substituted catechols. *Environ. Sci. Technol.* 52 (8), 4763–4773.
- von Gunten, U., 2003. Ozonation of drinking water: Part I. Oxidation kinetics and product formation. *Water Res.* 37 (7), 1443–1467.
- von Gunten, U., 2003. Ozonation of drinking water: Part II. Disinfection and by-product formation in presence of bromide, iodide or chlorine. *Water Res.* 37 (7), 1469–1487.
- von Gunten, U., 2018. Oxidation processes in water treatment: are we on track?. *Environ. Sci. Technol.* 52 (9), 5062–5075.
- Wenk, J., Aeschbacher, M., Salhi, E., Canonica, S., von Gunten, U., Sander, M., 2013. Chemical oxidation of dissolved organic matter by chlorine dioxide, chlorine, and ozone: effects on its optical and antioxidant properties. *Environ. Sci. Technol.* 47 (19), 11147–11156.
- Westerhoff, P., Yoon, Y., Snyder, S., Wert, E., 2005. Fate of endocrine-disruptor, pharmaceutical, and personal care product chemicals during simulated drinking water treatment processes. *Environ. Sci. Technol.* 39 (17), 6649–6663.
- Wu, J., Cheng, S., Cai, M.-H., Wu, Y.-P., Li, Y., Wu, J.-C., Li, A.-M., Li, W.-T., 2018. Applying UV absorbance and fluorescence indices to estimate inactivation of bacteria and formation of bromate during ozonation of water and wastewater effluent. *Water Res.* 145, 354–364.
- Yang, M., Zhang, X., 2013. Comparative developmental toxicity of new aromatic halogenated DBPs in a chlorinated saline sewage effluent to the marine polychaete *platynereis dumerilii*. *Environ. Sci. Technol.* 47 (19), 10868–10876.
- Young, T.R., Li, W., Guo, A., Korshin, G.V., Dodd, M.C., 2018. Characterization of disinfection byproduct formation and associated changes to dissolved organic matter during solar photolysis of free available chlorine. *Water Res.* 146, 318–327.